JACS
JOURNAL OF THE AMERICAN CHEMICAL SOCIETY
Article
pubs.acs.org/JACS

Electrochemical Evidence for Intermolecular Proton-Coupled Electron Transfer through a Hydrogen Bond Complex in a *p*-Phenylenediamine-Based Urea. Introduction of the "Wedge Scheme" as a Useful Means To Describe Reactions of This Type

Laurie A. Clare, An T. Pham, Francine Magdaleno, Jaqueline Acosta, Jessica E. Woods, Andrew L. Cooksy, and Diane K. Smith*

Department of Chemistry and Biochemistry, San Diego State University, San Diego, California 92182-1030, United States

Supporting Information

ABSTRACT: The electrochemistry of several *p*-phenylenediamine derivatives, in which one of the amino groups is part of an urea functional group, has been investigated in methylene chloride and acetonitrile. The ureas are abbreviated U(R)R′, where R′ indicates the substituent on the N that is part of the phenylenediamine redox couple and R indicates the substituent on the other urea N. Cyclic voltammetry and UV−vis spectroelectrochemical studies indicate that U(Me)H and U(H)H undergo an apparent 1e$^-$ oxidation that actually corresponds to 2e$^-$ oxidation of half the ureas to a quinoidal-diimine cation, U(R)$^+$. This is accompanied by proton transfer to the other half of the ureas to make the electroinactive cation HU(R)H$^+$. This explains the observed irreversibility of the oxidation of U(Me)H in both solvents and U(H)H in acetonitrile. However, the oxidation of U(H)H in methylene chloride is reversible at higher concentrations and slower scan rates. Several lines of evidence suggest that the most likely reason for this is the accessibility of a H-bond complex between U(H)$^+$ and HU(H)H$^+$ in methylene chloride. Reduction of the H-bond complex occurs at a less negative potential than that of U(H)$^+$, leading to reversible behavior. This conclusion is strongly supported by the appearance of a more negative reduction peak at lower concentrations and faster scan rates, conditions in which the H-bond complex is less favored. The overall reaction mechanism is conveniently described by a "wedge scheme", which is a more general version of the square scheme typically used to describe redox processes in which proton transfer accompanies electron transfer.

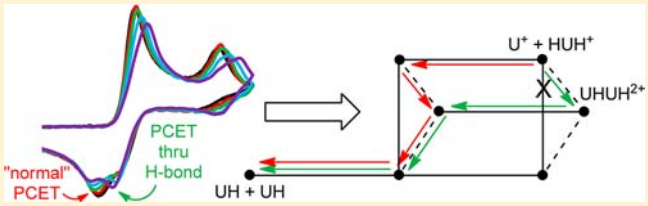

INTRODUCTION

There is a growing awareness of the important role that H-bond complexes can play in complex electron-transfer mechanisms. This is due in part to the current interest in the mechanism of proton-coupled electron transfer (PCET) reactions,[1−5] which arises both because of the importance of PCET in biological electron transfer[6−8] and because these reactions are central to nonthermal, fuel-consuming and producing processes, such as those involved in fuel cells or envisioned for artificial photosynthesis.[9] Until relatively recently, it had been thought that PCET reactions always proceeded stepwise with sequential electron and proton transfer. Much of the recent fundamental interest in PCET stems from the realization that a third option is available, concerted electron and proton transfer or "CPET" in which the electron and proton both move in a single kinetic step.[1−5,10] This focus on the concerted process has increased awareness of the importance of H-bond states in PCET, since the concerted reaction occurs within a H-bonded intermediate.[1−5,10] However, it is also recognized that even in the absence of CPET, H-bonding can have a substantial effect on the energetics of electron transfer,[11−23] or alternatively, electron transfer can have a substantial effect on the energetics of H-bonding. This latter realization has led to increased awareness of the importance of H-bonding in electron transfer from an entirely different front, namely, supramolecular chemistry. In this context, it is well recognized that H-bonds are one of the most important and useful intermolecular interactions for creating well-defined supramolecular complexes. With incorporation of reversible redox couples and proper design, electron transfer can provide a convenient means both to detect the H-bond complex and control its assembly.[24,25]

Our interest in H-bonding and electron transfer comes primarily from the latter, supramolecular perspective. Over the years, our group has introduced a number of simple supramolecular complexes in which the strength of H-bonding can be controlled electrochemically.[26−30] One such system, and the subject of this report, is the electroactive urea, U(H)H.[30] Ureas are very good H-donors and as such are often used in synthetic hosts. In general, incorporation of a reversible redox couple into a host can provide a means to detect the presence of guests through shifts in the redox potential brought about by guest binding.

Received: September 30, 2013
Published: November 27, 2013

   dx.doi.org/10.1021/ja410061x | J. Am. Chem. Soc. 2013, 135, 18930−18941

In the case of U(H)H, a *p*-dimethylamino group converts 1,3-diphenylurea into a *p*-phenylenediamine derivative. As expected for *p*-phenylenediamines, U(H)H undergoes a reversible oxidation in CH_2Cl_2, which we initially interpreted as the $1e^-$ oxidation to the radical cation. Addition of the cyclic diamide PZD results in significant negative shifts in the potential of the cyclic voltammetric (CV) wave of U(H)H, consistent with strong H-bonding to the oxidized urea, Scheme 1.

Scheme 1

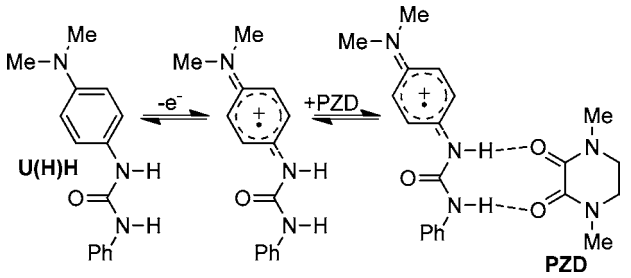

Shortly after our report on U(H)H, Sibert and co-workers published a closely related study in which they looked at redox-dependent anion binding with other phenylenediamine-based ureas.[31] Similar to our results, they observed large negative shifts in the redox potential of the ureas upon addition of anions, such as acetate, that can H-bond to the urea NHs. They also interpreted their results as being due to an increase in H-bond strength between the oxidized ureas and the guests. However, in their case, the observed negative shift in potential was also accompanied by a doubling in current, signaling a conversion from a $1e^-$ to $2e^-$ process. Such behavior, not discussed by the authors, is strongly indicative of proton transfer occurring and not merely H-bonding.

Although in our case the CV wave height does not change significantly upon addition of PZD, upon further analysis of the voltammetry of U(H)H at different concentrations in CH_2Cl_2 and in CH_3CN, and also by comparing its voltammetry to that of derivatives in which one or both urea N–H's are replaced by N-Me's, U(Me)H, and U(Me)Me, respectively, we now realize that proton transfer is occurring upon oxidation of the phenylenediamine ureas, even without added guest. Analysis of our more recent data leads to the conclusion that the NH protons in the radical cations of both U(H)H and U(Me)H are sufficiently acidic that they can be removed by the NMe_2 on another urea in its reduced state. The uncharged radical thus formed is easier to oxidize than the original urea, leading to immediate removal of a second electron to give the doubly oxidized quinoidal cation, $U(R)^+$, along with the now electrochemically inactive fully reduced, protonated urea, $HU(R)H^+$. Therefore, the overall reaction involves $2e^-$ oxidation of one urea and deactivation of another via protonation for a net $1e^-$ per urea, top reaction in Scheme 2.

The suggestion that the top reaction in Scheme 2 occurs with phenylenediamines is not new. Peculiarities in the voltammetry of NH-containing phenylenediamines in aprotic solvents have been noted, and we[32] and others[33,34] have suggested proton transfer as a possible explanation. However, a problem with this is the generally observed reversibility[35] of the first voltammetric wave for phenylenediamine oxidation, which is not expected when proton transfer accompanies electron transfer in organic solvents.[36−38] What is unique about this system is that with

Scheme 2

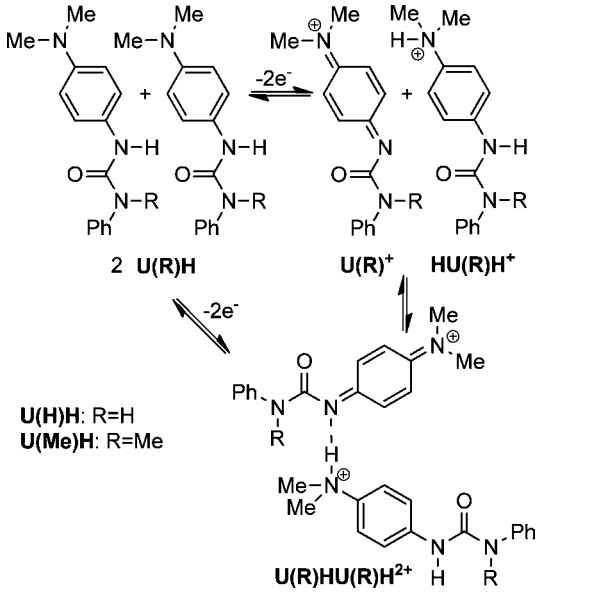

U(Me)H in both solvents, and U(H)H in CH_3CN, we actually do see the expected less than reversible behavior in the first CV wave, which makes the observed reversible behavior for U(H)H in CH_2Cl_2 more striking. The simplest explanation for this difference is the stability of the H-bond complex that can be formed between the products, Scheme 2. This will be greatest for U(H)H in CH_2Cl_2. Thus a reasonable explanation is that the observed reversibility is due to the H-bond complex providing a lower energy pathway for the reverse reduction.

Why is this a significant result? First, because the proposed mechanism is actually a more general mechanism for the classic $2e^-$, $1H^+$ "ECE" pathway that is generally thought to explain the $2e^-$ redox transformations observed in aqueous solution for quinones, phenylenediamines, and a variety of other organic redox couples with acid/base functionality. This is because proton transfer generally goes through a H-bond intermediate.[39,40] In most cases, the intermediate is sufficiently short-lived that it can be ignored, but if the conditions are such that it has sufficient stability that it cannot be ignored, then electron transfer to/from the H-bond intermediate can provide a lower energy pathway, *irrespective of whether the process is concerted or stepwise within the H-bonded complex*. Second, stability of the H-bond complex has largely been left out of the discussion of CPET, yet it is clearly of importance. Mader and Mayer made this same point in a recent study dealing with homogeneous CPET, where they noted that the energetics of the formation of the H-bonded precursor and successor complexes were actually the dominant contributors to the overall energetics.[41]

The development of a useful graphical representation to describe the proposed mechanism is outlined in Scheme 3 for the generic $1e^-$, $1H^+$ oxidation, $AH + B = A + HB^+ + e^-$. Such reactions are commonly described by square schemes as illustrated in Scheme 3a, with the two possible electron-transfer reactions shown on the horizontal axes and the two possible proton-transfer reactions shown on the vertical axes. The *overall* concerted reaction is indicated by the diagonal. The utility of this presentation is that it clearly defines the thermodynamic relationship between the five reactions. It also outlines the three pathways now believed to be generally possible for the overall reaction: (1) proton transfer followed by electron transfer or

dx.doi.org/10.1021/ja410061x | J. Am. Chem. Soc. 2013, 135, 18930−18941

Scheme 3. Development of the Wedge Scheme

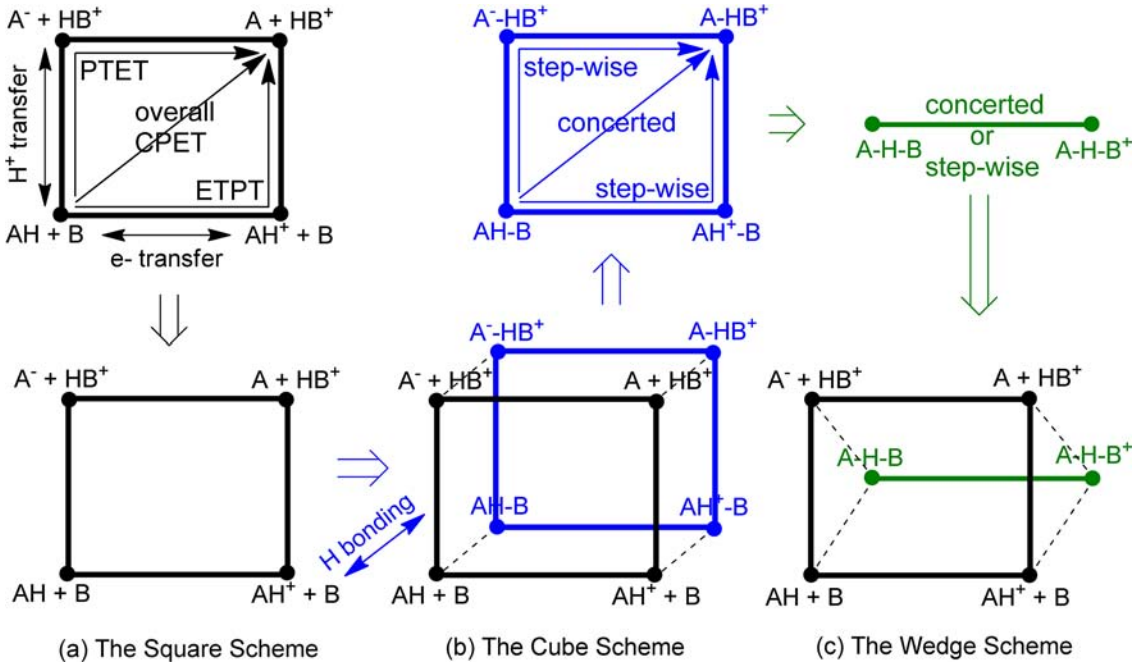

PTET; (2) electron transfer, followed by proton transfer or ETPT; and (3) concerted proton and electron transfer or CPET. While the diagonal in the square indicates the overall equation for the latter, in fact, as noted above, the actual concerted transfer occurs through a H-bond intermediate, as do the proton transfer reactions. Therefore, a more complete representation of the pathways requires another dimension to represent the H-bonding steps. This leads to the cube scheme, Scheme 3b. The back panel of the cube (in blue) represents the electron and proton transfer reactions within the H-bonding complex, and thus, the diagonal here represents the true concerted step, the E° of which is affected by the magnitudes of the K's for the H-bonding reactions and, unless they are all equal, will not be the same as the E° for the overall concerted reaction.

While the cube scheme provides a complete description of the intermediates (assuming only 1:1 H-bonding is important), from a kinetic, mechanistic view, it is also likely needlessly complex, since all the reactions in the back panel are unimolecular. As Laviron[42] pointed out for the normal square, Scheme 3a, if the proton transfers are at equilibrium, then the overall square behaves like a simple $1e^-$ transfer with an apparent E° that depends on the two-component E°'s and the two K's. Certainly, proton transfers will be at equilibrium within a H-bond complex. Thus, for kinetic evaluation of the *overall* mechanism, the back square can be replaced by a single electron transfer step (shown in green), giving a "wedge", Scheme 3c.

The wedge scheme consists of two triangular "sides" that describe the proton transfer, H-bond equilibria for each oxidation state and three square faces. The front square (bold black in Scheme 3c) represents the overall proton transfer, electron transfer equilibria. The bottom square (AH + B, A–H–B, A–H–B^+, AH^+ + B) describes the H-bond, electron transfer equilibria for the protonated state, and the top square (A^- + HB^+, A–H–B, A–H–B^+, A + HB^+) describes the H-bond, electron transfer equilibria for the deprotonated state.

Logically it makes sense that the E° of electron transfer within the H-bond complex should be in between that of the completely protonated and completely deprotonated forms. This can be confirmed by considering the relationship between the K's of the proton transfer steps or the H-bond steps and the E°'s for the three squares comprising the faces of the wedge. As outlined in the Supporting Information, this analysis leads to the conclusion that the order of E° values is $A^{-/0}$ < A–H–$B^{0/+}$ < $AH^{0/+}$, which has significant ramifications for the electrochemical reversibility of the AH,B/A,HB^+ redox couple. Since oxidation/reduction typically has a huge effect on acid/base character, there is often a very large difference between the E° values of the protonated and deprotonated species. Because of this, it is common for reactions that involve net transfers of electrons and protons to exhibit electrochemically irreversible voltammetric behavior,[35] with large ΔE_p values, since the potential required to add/remove the electron is so different in the starting and ending oxidation states. The existence of a relatively long-lived H-bond intermediate should improve the electrochemical reversibility by providing a pathway of intermediate potential.

The evaluation of the mechanism for the oxidation of U(H)H in CH_2Cl_2 provides strong evidence for the operation of a wedge scheme, particularly in the context of the different behavior observed in CH_2Cl_2 vs the more polar CH_3CN and in the different behavior observed for the more sterically hindered U(Me)H in both solvents. Part of the evidence is the greater voltammetric reversibility observed for U(H)H in CH_2Cl_2, but in addition we are able to clearly observe a concentration and scan rate dependent conversion between two different reduction pathways on the return scan. This behavior cannot be explained by a simple square scheme but is readily explained by the wedge scheme.

EXPERIMENTAL SECTION

Chemicals. HPLC-grade CH_2Cl_2 and CH_3CN were distilled over CaH_2 and collected under N_2. NBu_4PF_6 was recrystallized three times in 95% reagent alcohol and dried under vacuum overnight at 100 °C.

dx.doi.org/10.1021/ja410061x | J. Am. Chem. Soc. 2013, 135, 18930–18941

The ureas used in this study were synthesized as described in the Supporting Information.

General Voltammetry Procedures. Cyclic voltammetry (CV) experiments were performed using either a CH Instruments model 600c or 760d digital potentiostat. All experiments were conducted in 0.10 M NBu_4PF_6/CH_2Cl_2 or CH_3CN in a jacketed one-compartment electrochemical cell. For experiments conducted outside the glovebox, temperature was controlled using a circulating water bath to flow 25 °C water through the outer jacket of the cell. For all voltammetry experiments, a Pt disk working electrode (area = 0.028 cm^2), a Pt wire counter electrode and a Ag wire pseudoreference electrode placed in its own separate compartment were used. The working electrode was polished immediately prior to use with 1/4 μm diamond polishing paste (Buehler), washed thoroughly with water, then polished with 0.05 μm alumina paste (Buehler) and washed with water and acetone. To keep the electrochemical cell dry it was stored in an oven at 100 °C. Immediately after removal from the oven, the cell was placed under Ar and dry electrolyte added. The solvent was then passed through a column of activated alumina into the cell. For routine experiments, after background scans were recorded, the electroactive compound was added directly to the electrolyte solution in the cell. For experiments in which a more accurate concentration was needed, the solutions were prepared by first adding the electrolyte and the urea derivative into a volumetric flask. Solvent, which had been previously passed through a column of activated alumina, was then added to give a 1 mM solution of analyte. The solution was transferred by syringe to the electrochemical cell. A small steady flow of Ar through the cell was maintained throughout the experiment in order to help keep the solvent dry.

Cyclic Voltammetry Studies of U(H)H, U(Me)H, and U(Me)Me at Different Concentrations and Scan Rates. To minimize the effect of water on the electrochemistry, voltammetry studies on scan rate and concentration dependence were conducted in the same electrochemical cell in a N_2-atmosphere glovebox. This limited temperature control of the cell but minimized problems with solvent evaporation. To prepare very dry solvents, CH_3CN or CH_2Cl_2 was passed through an alumina column into a flask, transferred to the glovebox, then added to previously dried NBu_4PF_6. This solution was allowed to sit 48 h on 3A molecular sieves that had previously been activated by drying under vacuum at 250 °C for 12 h. U(H)H and U(Me)H were also vacuum-dried prior to being measured into a 1 mL flask that was then placed into the glovebox. Immediately before CV studies, a 7−10 mM stock solution of urea was made using the electrolyte solution dried on the molecular sieves.

In order to get stable backgrounds for reliable subtraction at the lowest concentrations, the electrode was cycled through the potential range a number of times until the charging currents stabilized. Typically this involved three sets of 20 cycles at 1 V/s. After the currents stabilized, background scans were recorded at 0.20, 0.50, 1.0, 2.0, and 5.0 V/s. An appropriate amount of the urea stock solution was then added using 10−100 μL gastight syringes to make solutions of approximately 0.04, 0.08, 0.16, 0.32, 0.64, and 1.2 mM urea. The urea concentrations were corrected for the change in volume assuming the volume was additive and no evaporation. After each addition, CV's were recorded at 0.20, 0.50, 1.0, 2.0 and 5 V/s. A number of the low concentration, fast scan rate CV's obtained in the glovebox showed significant 60 MHz noise. This was removed from the data using the IIR notch filter in the Igor Pro v6.10a software package.

CV simulations. The background-subtracted CV's for U(H)H in CH_2Cl_2 were fit to the "wedge scheme" mechanism given in Table 1 using the Digisim CV simulation software (v 3.03, BioAnalytical Systems) and Butler−Volmer kinetics. Note that the equilibrium constants for the proton-transfer reactions in this mechanism were included in order to set the other equilibria, but the rate constants were set to zero with the assumption that the proton transfer proceeds through the H-bond intermediate. In order to minimize interference from the oxidation of another species that shows up at higher concentrations and slower scan rates (vide infra), only the CV's at lower concentrations and faster scan rates were used for the fittings (a total of 16 CV's). The simulations assumed an uncompensated resistance of 1900 Ω. This value was calculated using $R = \rho/(4r)$,[43] a resistivity (ρ) of 720 Ω cm for 0.1 M NBu_4PF_6/CH_2Cl_2 at 25 °C,[44] and an electrode radius (r) = 0.094 cm. A large number of preliminary simulations were run prior to the fitting process in order to determine reasonable starting values for the K's and for the standard electron-transfer rate constants, $k°$. The starting values for the k_f's of the H-bonding reactions were set close to the diffusion controlled limit at 1×10^8 M^{-1} s^{-1}. The α values for all the electron transfers were set to 0.5, and the diffusion coefficients, D, of all species were linked to that of U(H)H, with a starting value of 1×10^{-5} cm^2 s^{-1}. An iterative procedure was used for the fittings: first the K's were optimized, followed by the $E°$'s, the $k°$'s and finally the k_f's. The cycle was then repeated until no significant improvement was observed.

Table 1. Mechanism Used To Fit the CVs of U(H)H in CH_2Cl_2 and Resulting Best-Fit Kinetic and Thermodynamic Parameters

reaction	final $E°$[a] (K)	final $k°/k_f$
$UH^+ + e = UH$	0.10 V	0.11 cm/s
$UH^{2+} + e = UH^+$	0.62 V	0.0044 cm/s
$U^+ + e = U$	(−0.08 V)	0.044 cm/s
$UHUH^{2+} + e = UHUH^+$	0.08 V	0.69 cm/s
$UH^+ + UH = U + HUH^+$	1.3×10^{-4}	0 M^{-1} s^{-1}
$UH^{2+} + UH = U^+ + HUH^+$	9.3×10^7	0 M^{-1} s^{-1}
$UH^+ + UH = UHUH^+$	8.7 M^{-1}	1.6×10^7 $M^{-1}s^{-1}$
$UH^{2+} + UH = UHUH^{2+}$	(1.8×10^{10} M^{-1})	3.6×10^7 $M^{-1}s^{-1}$
$U + HUH^+ = UHUH^+$	(6.9×10^4 M^{-1})	1×10^{10} $M^{-1}s^{-1}$
$U^+ + HUH^+ = UHUH^{2+}$	(200 M^{-1})	1.1×10^6 $M^{-1}s^{-1}$

[a]Values in parentheses are thermodynamically redundant and so were set by the other parameters.

Spectroelectrochemical Studies. Spectroelectrochemical experiments were conducted using a Cary Bio 50 UV−vis spectrometer and a homemade optically transparent thin layer electrochemical (OTTLE) cell. Details on its construction and use are provided in the Supporting Information.

RESULTS AND DISCUSSION

Voltammetric and Spectroelectrochemical Evidence for Proton Transfer upon Oxidation of the Ureas in CH_3CN and CH_2Cl_2. Figure 1 shows concentration-normalized cyclic voltammograms (CV's) of U(Me)Me, U(H)H, and U(Me)H in CH_2Cl_2 using the same Pt working electrode at 0.2 V/s. Despite the similarities in structure, all the ureas show clearly different voltammetric behavior. U(Me)Me, scan (a) in black, is the only one that shows the generally expected behavior for phenylenediamines in aprotic solvents—two reversible oxidations.[32,45,46] The first, at 0.13 V vs Fc, corresponds to the $1e^-$ oxidation to the radical cation, followed by the second, at 0.67 V vs Fc, corresponding to the $1e^-$ oxidation of the cation to the quinoidal diimine dication, Scheme 4.

Like U(Me)Me, U(H)H also shows two CV waves in CH_2Cl_2, scan (b) in red in Figure 1. The first is reversible and appears to be due to a $1e^-$ process as judged by how close in height it is to the U(Me)Me CV waves. A second CV wave for U(H)H is also observed at more positive potentials, although in contrast to the second U(Me)Me CV wave, the second U(H)H wave is not chemically reversible and shows an unusual shape that is not consistent with simply an irreversible $1e^-$ wave.

U(Me)H, scan (c) in blue in Figure 1, shows yet a different type of CV behavior. The first oxidation peak is the same height as that of U(Me)Me, again suggesting a $1e^-$ oxidation, but there is only a hint of a second oxidation at the potential it would be expected. Furthermore, the first oxidation is only

dx.doi.org/10.1021/ja410061x | J. Am. Chem. Soc. 2013, 135, 18930−18941

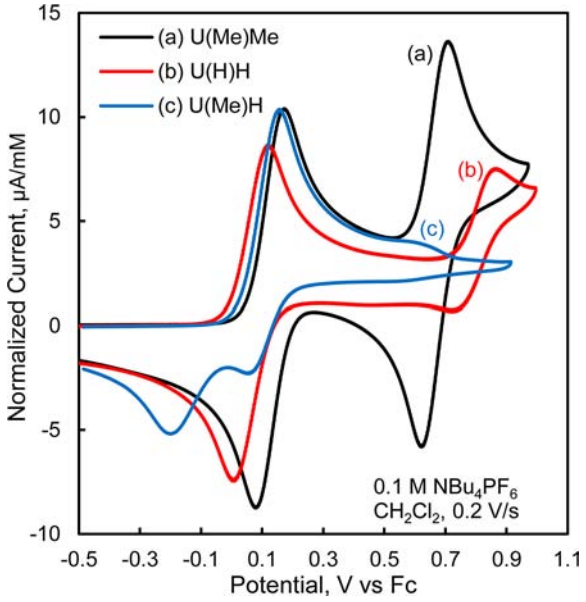

Figure 1. CV's (0.2 V/s) in 0.1 M NBu_4PF_6/CH_2Cl_2 of (a) 0.5 mM U(Me)Me, (b) 1 mM U(H)H, and (c) 1 mM U(Me)H. The current has been normalized by dividing by concentration in mM.

Scheme 4

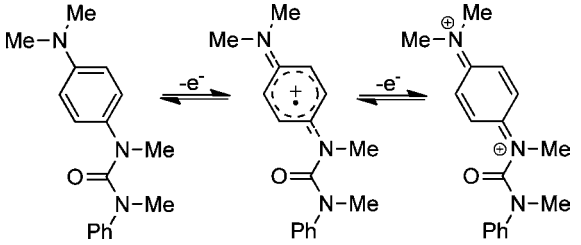

partially chemically reversible[35] with a small return peak. The major peak on the return scan occurs ~0.3 V negative of the forward oxidation peak. This voltammetry suggests a "square-scheme" type mechanism where the initially formed product converts to something else that is more difficult to reduce.

Figure 2 shows CV's of the same species in Figure 1 except in CH_3CN. Both U(Me)Me, scan (a) in black, and U(Me)H, scan (b) in blue, show similar CV behavior in CH_3CN as CH_2Cl_2, but U(H)H, scan (c) in red, does not. Whereas U(H)H appears to undergo a reversible $1e^-$ oxidation in CH_2Cl_2, the first oxidation is not chemically reversible in CH_3CN, displaying a negatively shifted return peak similar to that seen for U(Me)H in both solvents. Furthermore, the second oxidation wave observed in CH_2Cl_2 is now gone, so overall the CV behavior for U(H)H in CH_3CN is very similar to that observed for U(Me)H.

Insight into the origin of the urea CV behavior is provided by addition of pyridine, shown for U(H)H in CH_2Cl_2 in Figure 3. Addition of 1 equiv of pyridine causes a significant increase in the current of the reversible wave, peaks Ia/Ic, along with the elimination of the small irreversible oxidation wave, peak IIa, and the appearance of a new broad, quasi-reversible wave, peaks IIIa/IIIc. As the amount of pyridine is increased, the reversible wave, Ia/Ic, increases further in height and the broad wave, IIIa/IIIc, disappears. At 16 equivalents of pyridine, the first wave, Ia/Ic, has almost doubled in height, but is still reversible. Similar behavior is seen with U(H)H in CH_3CN, Figure 4,

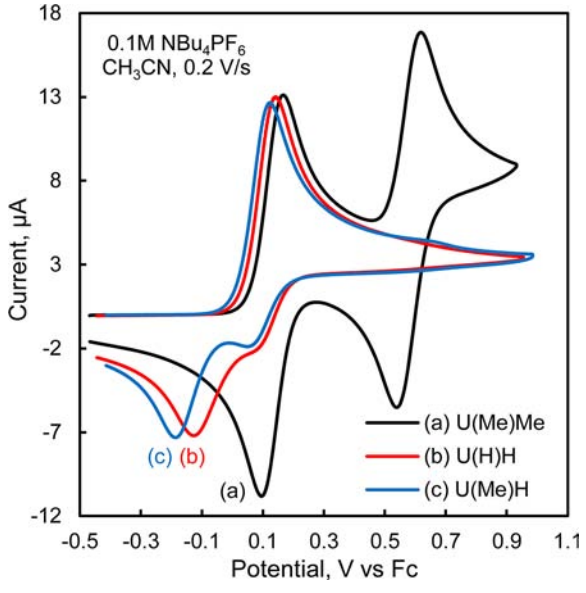

Figure 2. CVs (0.2 V/s) in 0.1 M NBu_4PF_6/CH_3CN of (a) 1 mM U(Me)Me, (b) 1 mM U(H)H, and (c) 1 mM U(Me)H.

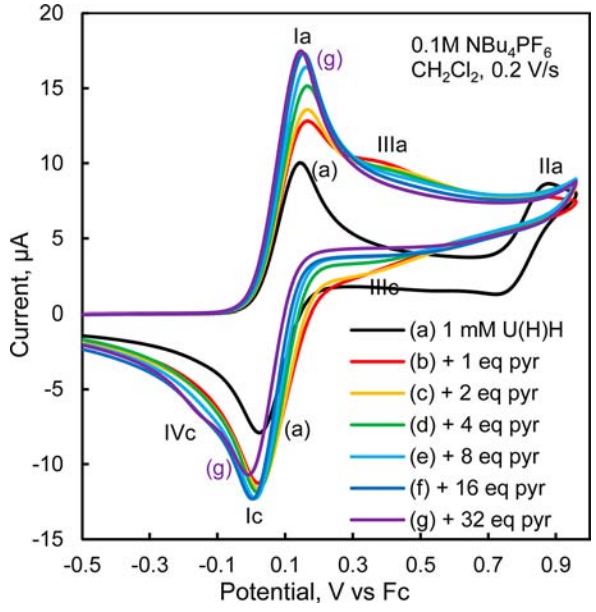

Figure 3. CV's (0.2 V/s) of 1 mM U(H)H in 0.1 M NBu_4PF_6/CH_2Cl_2 with different equivalents of pyridine.

except the CV wave is not chemically reversible to begin with and stays so as pyridine is added and the current increases. The effect of adding pyridine to U(Me)H in both solvents is very similar to that seen in Figure 4. (See Figure S1 in the Supporting Information.)

The behavior observed for both ureas upon addition of pyridine is consistent with pyridine being a strong enough base to deprotonate the urea radical cation, $U(R)H^+$. This gives the uncharged radical, U(R), which should be easier to oxidize than the starting urea leading to immediate removal of a second electron to give the quinoidal cation, $U(R)^+$, and an overall $2e^-$ oxidation, eqs 1–3, where B is pyridine.

$$U(R)H - e^- = U(R)H^+ \quad (1)$$

$$U(R)H^+ + B = U(R) + HB^+ \quad (2)$$

dx.doi.org/10.1021/ja410061x | J. Am. Chem. Soc. 2013, 135, 18930–18941

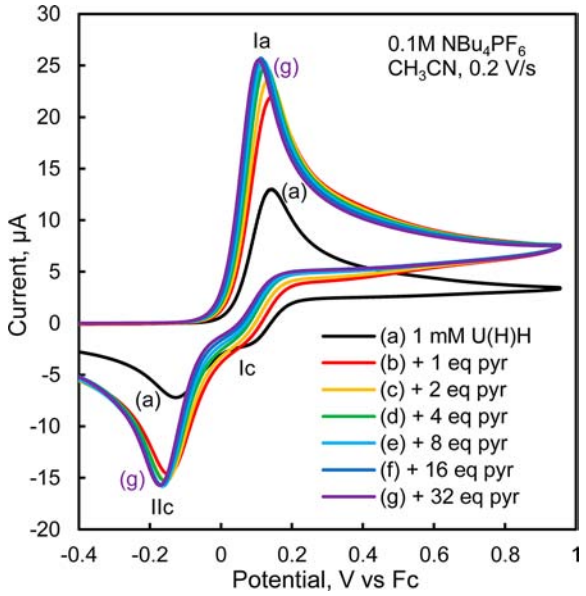

Figure 4. CVs (0.2 V/s) of 1 mM U(H)H in 0.1 M NBu_4PF_6/CH_3CN with different equivalents of pyridine.

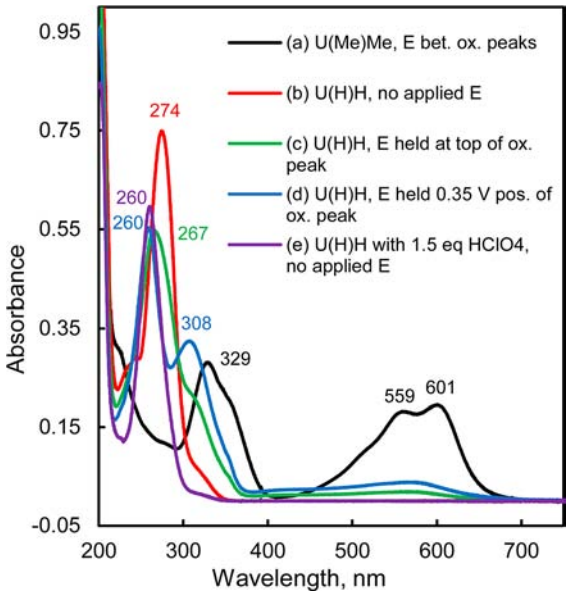

Figure 5. UV–vis spectroelectrochemical data in 0.1 M NBu_4PF_6/CH_3CN for (a) 0.5 mM U(Me)Me and (b–d) 0.5 mM U(H)H. (e) Spectrum for 0.5 mM U(H)H with 1.5 equiv of $HClO_4$.

$$U(R) - e^- = U(R)^+ \quad (3)$$

The relevance of this to the CV's with no pyridine is that the basicity of the dimethylamino group on the urea should be very close to that of pyridine.[47] Thus if pyridine can deprotonate the urea radical cation, another unoxidized urea ought to be able to do so as well. Indeed, addition of *N*,*N*′-dimethylaniline also causes an increase in the current of urea oxidation, although the behavior is more difficult to interpret since *N*,*N*′-dimethylaniline is oxidized itself at a potential just a little more positive than the urea. (See Figure S2 in the Supporting Information.) Nonetheless, the data suggest that another urea should be able to deprotonate the radical cation, triggering the removal of the second electron, eqs 1–3, where B is now the starting urea, U(R)H. In this case, even though a $2e^-$ oxidation is occurring, the overall process appears to be $1e^-$ because the urea that takes the proton is no longer electroactive, making the overall reaction $1e^-$ per urea, Scheme 2. In this regard it is important to note that while addition of pyridine causes the current to increase, it does not have much effect on the wave shape, suggesting that a similar redox process is occurring both with and without pyridine.

Additional support for Scheme 2 comes from UV–vis spectroelectrochemical studies of U(Me)Me and U(H)H in CH_3CN. Representative results are shown in Figure 5. Spectrum (a) in black is that obtained with U(Me)Me held at a potential between the two oxidation waves. The observed spectrum is typical for phenylenediamine radical cations showing a peak in the near UV at 329 nm and a very broad, intense visible absorption with two maxima at 559 and 601 nm.[32,48−50] Spectra (b–e) are with U(H)H. The starting (reduced) urea, spectrum (b) in red, shows one major absorption at 274 nm. Oxidation of the urea produces spectrum (c), green, when the potential is held at the top of the oxidation peak, and spectrum (d), blue, when the potential is held 0.35 V past the peak. From spectrum (d), the oxidation product(s) show major absorptions in the UV at 260 and 308 nm, along with a weak, very broad visible absorption. The key point here is that the spectrum of the oxidation product(s) does not match that expected for the radical cation. Furthermore, addition of 1.5 equiv of $HClO_4$ to give the protonated, reduced urea, $HU(H)H^+$ results in spectrum (e), purple, which shows a major absorption peak at 260 nm. This matches the short wavelength absorption observed for the oxidized product(s) in spectrum (d). Thus, spectrum (d) appears to be a mixture of protonated reduced urea and some other product that is not the radical cation, consistent with Scheme 2.

Given the similarity of the CV's of U(H)H in CH_3CN and U(Me)H in both solvents, it would seem likely that they all undergo the same redox process, and based on the above considerations, that process is best described by Scheme 2. The irreversibility observed in the CV's is also consistent with this reaction because reduction of the quinoidal cation would be expected to occur at a potential more negative than that of the radical cation.

But what about U(H)H in CH_2Cl_2? Unlike the other cases, the oxidation appears reversible. There is also the small oxidation wave at more positive potentials. One hypothesis to explain the voltammetry would be that the self-deprotonation described above is not occurring for U(H)H in CH_2Cl_2 and that the first CV wave is as we originally thought it to be, the reversible $1e^-$ oxidation of U(H)H to the radical cation. The second CV wave could then be due to oxidation of the radical cation. As shown in Figure 3, addition of pyridine does cause that small second wave to disappear along with the increase in current. However, it is noteworthy that the first CV wave remains reversible at the lower concentrations of pyridine, even as the current doubles. Thus it would seem that the $2e^-$, $1H^+$ oxidation of U(H)H can be reversible in CH_2Cl_2.

The conclusion that the $2e^-$, $1H^+$ oxidation is also occurring with U(H)H in CH_2Cl_2 is further supported by the spectroelectrochemical data in that solvent, Figure 6. As in CH_3CN, the spectrum of the U(Me)Me radical cation, spectrum (a) in black, shows the double hump visible absorption typical for phenylenediamine radical cations. However, holding the potential at oxidizing potentials, spectra (c) in green and (d) in blue, produces a species with a broad

dx.doi.org/10.1021/ja410061x | J. Am. Chem. Soc. 2013, 135, 18930−18941

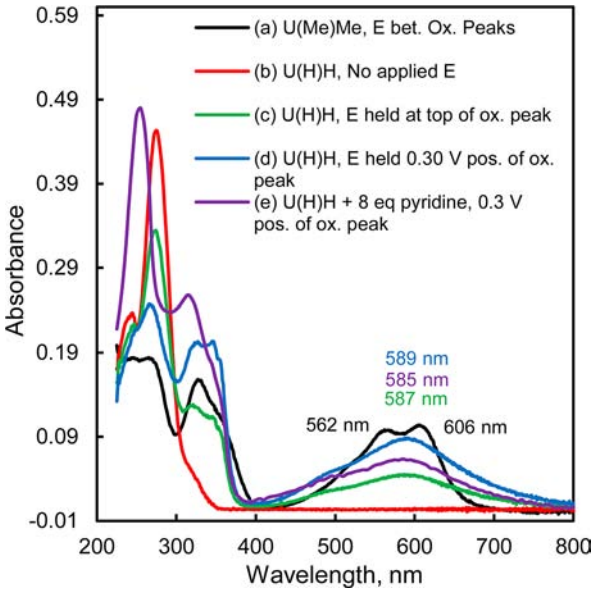

Figure 6. UV−vis spectroelectrochemical data in 0.1 M NBu_4PF_6/CH_2Cl_2 for (a) 0.5 mM U(Me)Me and (b−d) 0.5 mM U(H)H. (e) Spectrum for 0.5 mM U(H)H + 8 equiv of pyridine with the working electrode held 0.30 V past the oxidation peak.

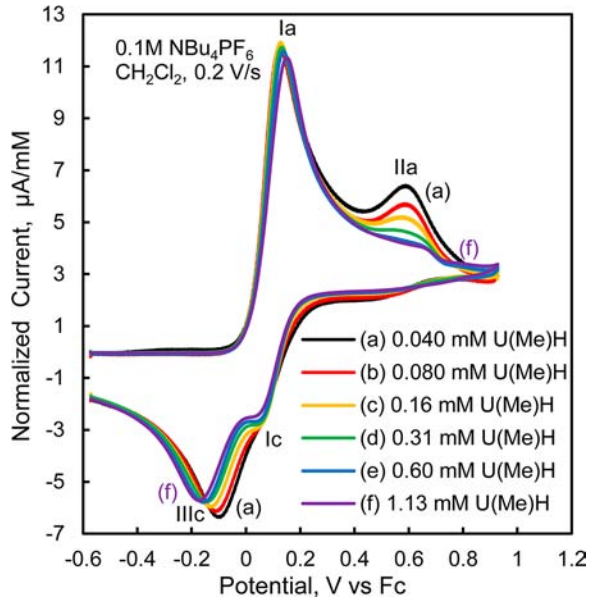

Figure 7. CVs (0.2 V/s) in 0.1 M NBu_4PF_6/CH_2Cl_2 with different concentrations of U(Me)H. The CVs have been background subtracted and normalized by dividing the current by concentration.

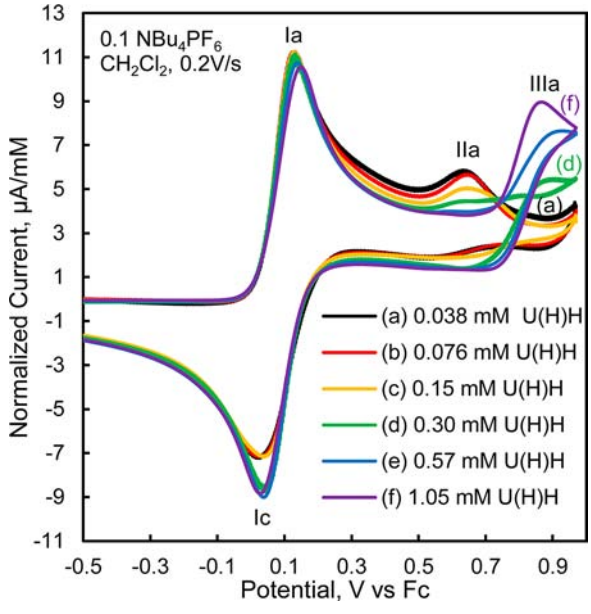

Figure 8. CVs (0.2 V/s) in 0.1 M NBu_4PF_6/CH_2Cl_2 with different concentrations of U(H)H. The CVs have been background subtracted and normalized by dividing the current by concentration.

visible absorption that does not match that expected for the radical cation. The visible absorption is more intense than that seen in CH_3CN, however any doubts to its origin are erased by doing the same experiment in the presence of 8 equivalents pyridine, spectrum (e), purple. Under these conditions, the CV's clearly indicate that the $2e^-$ oxidation is taking place, yet we see the same visible absorption as we do without pyridine.

As to the small irreversible wave observed for U(H)H in CH_2Cl_2, there are several additional clues that this is not due to the oxidation of the radical cation. In addition to its small size and unusual shape, scanning further positive shows additional oxidation processes that would not be expected for the quinoidal dication. (See Figure S3 in the Supporting Information.) More definitive proof, along with additional support for Scheme 2, comes from looking at the concentration dependence of the CV's and comparing this to that of U(Me)H, Figures 7 and 8. Since current is directly proportional to concentration, the currents in these plots have been normalized by dividing by concentration. These CV's were also obtained under very dry conditions in a glovebox, since we noted that the amount of water present affects the CV's at low concentrations of U(H)H.

Looking first at the concentration-dependent CV's of U(Me)H in CH_2Cl_2, Figure 7, there is a second oxidation peak, labeled IIa, that is clearly visible at lower concentrations. Peak IIa decreases with concentration such that it essentially disappears at the 1 mM concentration shown in Figure 1. Based on the U(Me)Me CV, this peak is at the right potential for oxidation of the radical cation. So, consistent with the bimolecular nature of Scheme 2, by going to a lower concentration it appears it is possible to partially outrun the proton transfer, leading to the appearance of the "missing" second oxidation wave. That this wave is completely irreversible is not surprising given that the dication has to be considerably more acidic that the radical cation.

Figure 8 shows the same type of concentration dependent study for U(H)H in CH_2Cl_2. The unusual shaped second oxidation wave noted earlier is present, labeled IIIa, but only at the higher concentrations. In fact, at the lower concentrations, the CV on the forward scan looks very similar to that seen for U(Me)H with a small irreversible oxidation wave, peak IIa, which decreases as the concentration increases. Again, the potential of peak IIa is around that expected for oxidation of the radical cation based on the CV of U(Me)Me. The first sign of peak IIIa is not seen until about 0.3 mM. As the concentration is increased peak IIa disappears and peak IIIa grows in. The sigmoidal shape of the new peak, particularly obvious at 0.6 mM, is characteristic of a CE process (chemical reaction, followed by electron transfer). This indicates that it is not simply due to oxidation of the radical cation, but instead is due

dx.doi.org/10.1021/ja410061x | J. Am. Chem. Soc. 2013, 135, 18930−18941

to oxidation of a species formed at higher concentrations. Thus, all indications are that the first oxidation wave for U(H)H in CH_2Cl_2, peak Ia, corresponds to same $2e^-$, $1H^+$ process as seen for U(H)H in CH_3CN and for U(Me)H in both solvents.

H-Bonding As an Explanation for the Reversibility of the $2e^-$,$1H^+$ Oxidation of U(H)H in CH_2Cl_2. For the $2e^-$, $1H^+$ oxidation of U(H)H in CH_2Cl_2 to appear reversible as seen in Figures 1, 3, and 8 and follow a proton transfer only mechanism, the proton transfer would have to be exceedingly fast. However, it is unlikely that a bimolecular proton transfer reaction involving N–H's would be faster in CH_2Cl_2 than CH_3CN. Indeed, the reaction would likely be close to diffusion-controlled in both solvents. What is likely is that a H-bond between the pyridinium or the protonated urea, $HU(H)H^+$, and the quinoidal urea N would be stronger in the less polar CH_2Cl_2. Formation of such a H-bonded complex would increase the rate of proton transfer by increasing the effective concentration of the acid. It also makes a CPET step possible, but, even without this, it would facilitate the reverse electron transfer reduce, since it would be easier to reduce the H-bonded quinoidal cation than the non-H-bonded cation.

The hypothesis that a H-bond complex is behind the reversibility observed for the oxidation of U(H)H in CH_2Cl_2 is also consistent with the structural perturbation introduced by replacing the other H with a Me group as in U(Me)H. Due to hindered rotation about the N to carbonyl C bond, ureas, like amides, have strong conformational preferences. Literature precedent,[51−53] supported by DFT calculations described in the Supporting Information, indicate that the U(H)H-derived quinoidal cation should prefer the "cis–cis" conformation shown below, whereas the U(Me)H-derived quinoidal cation should strongly prefer the "trans-cis" conformation. Thus, the N which must regain the proton upon reduction is located in a much more sterically hindered site in $U(Me)^+$ than $U(H)^+$, making formation of a H-bonded complex between this N and the acidic N–H on either pyridinium or protonated urea, $HU(R)H^+$, less favored with $U(Me)^+$ than $U(H)^+$.

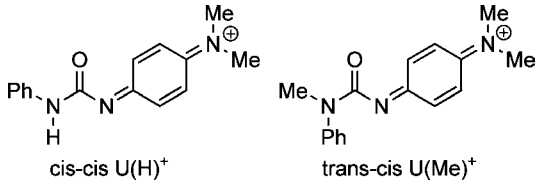

DFT calculations were also done to investigate possible structures of H-bond complexes formed between the protonated reduced urea and the quinoidal cation. Given these are gas-phase calculations, we initially thought the molecules would simply move apart due to the electrostatic repulsion. However, to our surprise, the geometry optimizations did reveal a complex that contains an H-bond between the acidic H on the dimethylamino of the reduced urea and the carbonyl O of the quinoidal urea. (See Figure S10c in Supporting Information.) This is presumably not the H-bond complex that would lead to the observed reversible electrochemistry, but it points out the fact that there are likely multiple H-bonded complexes possible in simple systems such as these.

Based on the above considerations, we formulated our hypothesis that H-bonded intermediates between the proton transfer partners need to be explicitly considered to explain the self-PCET reaction occurring with the ureas, resulting in the "wedge" scheme described in the Introduction. This is shown specifically for the urea oxidation in Scheme 5b, which can be compared to the corresponding square, Scheme 5a. Based on

Scheme 5. (a) Traditional Square Scheme for Urea Oxidation. (b) Wedge Scheme for Urea Oxidation

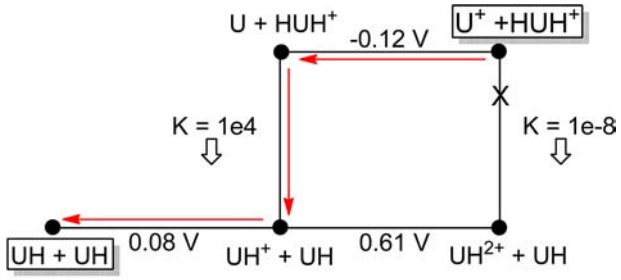

(a) Proton-transfer-only Square Scheme

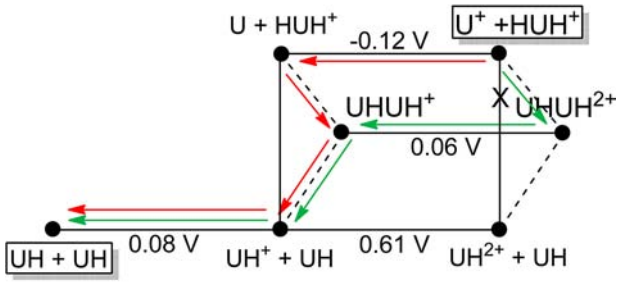

(b) Proton-transfer/H-bond Wedge Scheme

the experimental CV's, some initial estimates of the thermodynamic parameters can be made. Using data for U(H)H in CH_2Cl_2, $E°$ of $UH^{0/+}$ is 0.08 V vs Fc. The difference in $E_{1/2}$ between the two oxidation waves with U(Me)Me is 0.53 V, so assuming a similar difference with U(H)H, $E°$ of $UH^{+/+2}$ is ~0.61 V vs Fc. In order to obtain a $2e^-$ wave, the potential of the two electron transfers has to be inverted, which for an oxidation means the second electron transfer has to occur at a less positive potential. An inversion of −0.2 V is consistent with where the major return peak shows up with U(Me)H, giving a rough estimate of the $E°$ of $U^{0/+}$ as −0.12 V vs Fc. The values of E° of $UH^{+/2+}$ and $U^{0/+}$ set the ratio of the K's for the two proton-transfer reactions on the sides of the square (eq S1 in the Supporting Information). From the estimated $E°$'s, K_{PT} of the UH^{2+} proton transfer has to be about 10^{12} larger than that of UH^+. Since it appears to be reasonably easy (vide infra) to at least partially outrun the proton transfer reaction, K_{PT} of UH^+ has to be small, but it cannot be too small or the proton transfer would not occur to the extent it apparently does. Initial trial simulations of the voltammetry suggested a value of around 10^{-4} is reasonable, which means that K_{PT} of UH^{2+} is still very large, 10^8.

The significance of this for the proton-transfer-only square scheme mechanism is that the reverse reaction only has one readily available pathway, marked by the red arrows in Scheme 5a. This is because the large K_{PT} for UH^{2+} (10^8) means the reverse proton transfer is very unfavorable (10^{-8}) so even with a very fast forward rate, the reverse proton transfer will have to be fairly slow. In contrast, consideration of the H-bonded intermediate as in the wedge scheme opens up another possibility for the reverse reaction, indicated by the green arrows in Scheme 5b. The unfavorable reverse proton transfer reaction is broken into two reactions, so even though the

dx.doi.org/10.1021/ja410061x | J. Am. Chem. Soc. 2013, 135, 18930−18941

overall reverse proton transfer is very unfavorable, it is not necessarily unfavorable to form the H-bond complex. There is also an inherent concentration dependence to the equilibria forming the H-bond complex (due to the 2 going to 1 stoichiometry of the reaction) that is not present in the proton transfer reaction (2 going to 2 stoichiometry), with higher concentrations shifting the equilibrium position toward the complex. As noted in the Introduction, the E° of the H-bond complex will be between that of the other two electron transfers in the wedge, thus reduction of the complex will be easier than that of U^+, thereby creating an easier pathway for the reverse reaction. Strong evidence for this happening in the urea system comes from comparing the concentration and scan rate dependencies of the CV's of the different ureas.

Concentration and Scan Rate Dependence of the CV's. As with the single concentration, single scan rate CV's shown in Figures 1 and 2, the behavior of the multiple concentration and scan rate CV's can be largely grouped into two categories, the first comprising U(H)H in CH_3CN and U(Me)H in CH_2Cl_2 and CH_3CN and the second comprising U(H)H in CH_2Cl_2. Starting with the first grouping, the normalized, concentration-dependent CV's for U(Me)H and U(H)H in CH_3CN show features similar to the previously discussed concentration dependence of U(Me)H in CH_2Cl_2, Figure 7. These features include either extra current or a definite peak for oxidation of the radical cation at lower concentrations, and a return peak for reduction of the quinoidal cation that shifts more negative as the concentration increases for U(Me)H in CH_2Cl_2 and U(H)H in CH_3CN. With U(Me)Me in CH_3CN, the potential for reduction of the quinoidal cation is independent of concentration. (See Figures S4 and S5 in the Supporting Information.)

The effect of scan rate on the voltammetry of U(Me)H and U(H)H in CH_3CN and U(Me)H in CH_2Cl_2 is also quite similar. The scan rate dependence shown in Figure 9 of 0.15 mM U(Me)H in CH_2Cl_2 is representative. (Scan rate dependences of the other cases are shown in Figure S6 in the Supporting Information.) Since diffusion-controlled current increases with the square root of scan rate, the currents in this figure have been normalized by dividing by the square root of the scan rate. At the fastest scan rate of 5 V/s, the second oxidation, peak IIa, is clearly present, but this decreases in size as the scan rate slows and more time is available for proton transfer to occur at the radical cation stage. In addition, the peak for reduction of the quinoidal cation, IIIc, moves positive as the scan rate slows. This is consistent with a following reaction that removes the product of the electron transfer, shifting the equilibrium of electron transfer to a less extreme potential in the process. In this case the following reaction would be back proton transfer, the reverse of eq 2, followed by a second electron transfer, the reverse of eq 1, and return to the original oxidation/protonation state of the urea.

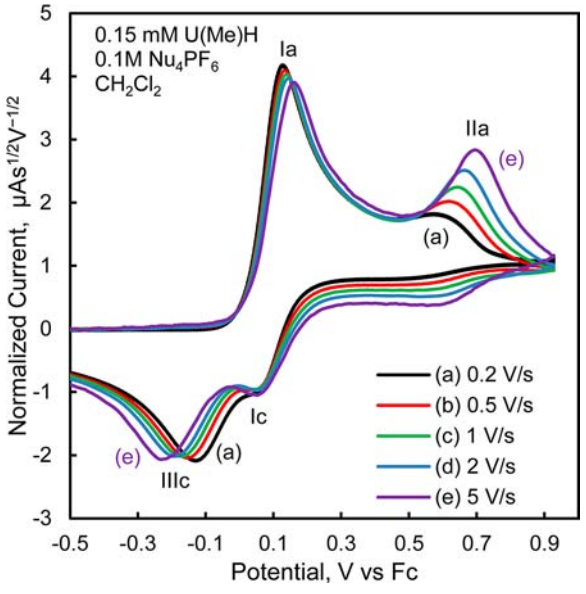

Figure 9. CVs of 0.15 mM U(Me)H in 0.1 $MNBu_4PF_6/CH_2Cl_2$ at different scan rates. CVs have been background subtracted and the currents normalized by dividing by square root of the scan rate.

The general features observed in the voltammetry of U(Me)H in both solvents and U(H)H in CH_3CN are qualitatively compatible with both the square and wedge schemes following the red pathway on the reverse scan, Scheme 5. An exception is the negative shift in the potential of the major reduction peak with increasing concentration that is observed for U(Me)H in CH_2Cl_2 and U(H)H in CH_3CN. We do not have a fully satisfactory explanation for this behavior at present. However, computer simulations show that the voltammetry of U(Me)H in CH_3CN is well accounted for by a proton-transfer only square scheme mechanism, Scheme 5a, with the inclusion of eqs 4 and 5. (See Table S1 and Figure S7 in the Supporting Information.)

$$U(Me)H^{2+} = U(Me)^+ + H^+ \quad (4)$$

$$U(Me)H + H^+ = HU(Me)H^+ \quad (5)$$

While U(Me)H in both solvents and U(H)H in CH_3CN show generally similar voltammetric behavior, which appears to be largely accounted for by the proton transfer square scheme, U(H)H in CH_2Cl_2 shows very different behavior that cannot be accounted for by proton transfer alone. At slow scan rates only one reduction peak is observed on the return scan at all concentrations studied, Figure 8. However, at faster scan rates the one reduction peak splits into two peaks as shown in Figure 10a. As the concentration increases, the more positive peak, peak Ic′, becomes relatively larger. This behavior is distinct from that of the other cases, where both at slow and fast scan rates (Figure 7 and Figures S4 and S5 in the Supporting Information) there is a small wave for reduction of residual radical cation and only one wave for reduction of the main oxidation product. The potential of this peak may change with concentration, but its relative intensity does not vary significantly, indicating there is primarily one pathway for the reduction. In contrast the two peaks with changing relative height observed for U(H)H at fast scan rates indicates that there are at least two pathways for the reduction with the easier, less negative one more available at higher concentration, just as predicted by the wedge scheme.

A similar conclusion can be reached by looking at the scan rate dependence of U(H)H in CH_2Cl_2. This is shown in Figure 11a for 0.15 mM. There are clearly two peaks on the return scan at this concentration, and the relative height of these varies with scan rate. As the scan rate slows the height of the first, more positive peak increases at the expense of the second. Again, this contrasts with the behavior seen for the other cases, where the main effect of scan rate is on the peak potential of the second reduction peak (Figure 9 and Figure S6 in the Supporting Information).

dx.doi.org/10.1021/ja410061x | J. Am. Chem. Soc. 2013, 135, 18930−18941

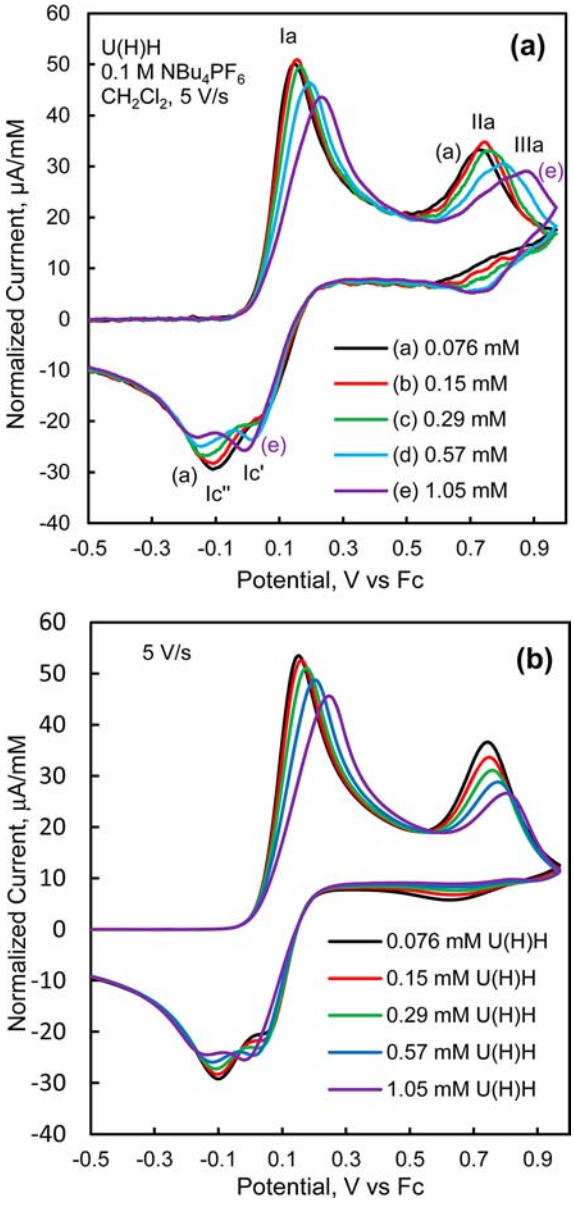

Figure 10. (a) Experimental and (b) simulated CV's (5 V/s) in 0.1 M NBu_4PF_6/CH_2Cl_2 with different concentrations of U(H)H. The CVs have been background subtracted and normalized by dividing the current by concentration. The mechanism and simulation parameters are given in Table 1.

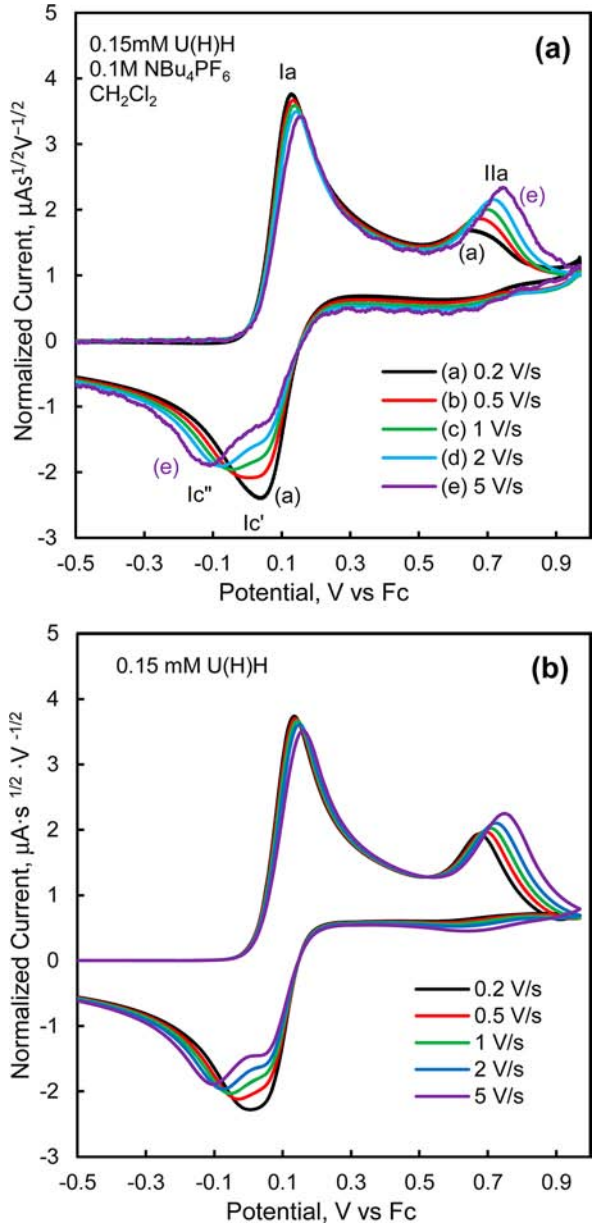

Figure 11. (a) Experimental and (b) simulated CV's of 0.15 mM U(H)H in 0.1 M NBu_4PF_6/CH_2Cl_2 at different scan rates. CVs have been background subtracted and the currents normalized by dividing by square root of the scan rate. The mechanism and simulation parameters are given in Table 1.

In order to test whether the wedge scheme mechanism can quantitatively account for the observed voltammetry of U(H)H in CH_2Cl_2, CV simulation software was used to fit the experimental voltammograms to this mechanism. The fittings were limited to the lower concentration, faster scan rate data in order to minimize interference from the small, second wave that grows in at higher concentrations. The thermodynamic and kinetic parameters corresponding to the best fit results are provided in Table 1, and simulated CV's presented in the same format as Figures 10a and 11a are given in Figures 10b and 11b, respectively. (Simulated CV's overlaid on top of the experimental CV's are given in Figure S8 in the Supporting Information.) Comparison of the two sets shows that the simulation clearly reproduces the major characteristics of the experimental CV's, with two overlapping reduction peaks on the return scan that change in relative height as the concentration and scan rate change. The fits are not perfect, but that is to be expected given that we have made no attempt to fit the second oxidation process that grows in at higher concentration. There is also the very real possibility that multiple H-bonded complexes are involved as suggested by the DFT calculations; thus, the wedge scheme, as complicated as it might seem, is almost certainly a simplification of the actual reaction taking place.

■ CONCLUSIONS

Voltammetric and spectroelectrochemical investigation of the oxidation of the phenylenediamine-type redox couples in U(H)H and U(Me)H shows that they undergo an overall $2e^-$, $1H^+$ transformation to the quinoidal diimine cation with concomitant transfer of the proton to another urea in CH_3CN

dx.doi.org/10.1021/ja410061x | J. Am. Chem. Soc. 2013, 135, 18930−18941

and CH_2Cl_2. This renders the protonated urea electroinactive, thus giving an apparent $1e^-$ transformation, with half of the ureas oxidized by two electrons and the other half remaining reduced. Such behavior has been observed in other systems. The unusual result here is that with U(H)H in CH_2Cl_2 the process gives reversible voltammetry at higher concentrations. In contrast, with U(H)H in CH_3CN and U(Me)H in both solvents, the process appears irreversible as expected. The structural and solvent effects provide strong circumstantial evidence in support of H-bonding being at the origin of this difference, with electron transfer through a H-bonded intermediate providing an easier pathway for the reverse reaction, leading to the observed reversible voltammetric behavior with U(H)H in CH_2Cl_2.

In this work, we have also introduced the "wedge scheme" as a convenient way to organize the reactions involved when the H-bonded intermediates must be considered in PCET. The utility of the wedge scheme is that it highlights the thermodynamic relationships between the electron transfer, proton transfer and H-bonding steps just as the square scheme does for PCET reactions in which H-bonding intermediates are not important. Indeed, as pointed out in the Introduction, the wedge scheme really is just a more detailed version of the proton transfer square scheme, since proton transfer reactions proceed through a H-bonded intermediate. The need for one scheme or the other depends on the stability or lifetime of the H-bonded intermediates. If the lifetimes of the H-bonded intermediates are insignificant compared to the other species, then there is no need to consider them in the overall reaction, and the H-bonding steps just get folded into the proton transfer equilibria. However, if the H-bonded intermediates have a sufficient lifetime, then they can provide an alternative pathway for the electron transfer at a potential that is intermediate between that of the fully protonated, fully deprotonated states.

A large portion of recent experimental and theoretical work on PCET reactions has dealt with the role of H-bonded intermediates. However, most of the focus is on whether the proton−electron transfer is stepwise or concerted within the H-bond complex. In contrast, our focus in this work is on the overall reaction and whether the electron transfer occurs through the H-bonded intermediate or through the non-H-bonded intermediates. By exploring the concentration and scan rate dependence of U(H)H in CH_2Cl_2, we can access conditions in which both processes occur. This only works because the H-bond complex is not favored in this case, since, if it were, the reaction would always proceed through the H-bonded intermediate.[54] The key is that even though the complex is not favored, it is still accessible at concentrations and times available in the CV experiment. Thus, we have found a system which appears to bridge the gap between the two major routes for PCET, one in which the electron transfer occurs within the H-bond complex and the other where it occurs only in the fully deprotonated/protonated states.

■ ASSOCIATED CONTENT

Supporting Information

Additional CVs of U(H)H and U(Me)H under a variety of conditions, CV simulations of U(Me)H in CH_3CN and U(H)H in CH_2Cl_2, synthetic procedures, spectral data for U(Me)H, details on the UV−vis spectroelectrochemical cell, DFT-calculated geometries, and relative ΔG's of U(H)H and U(Me)H in all oxidation states. This material is available free of charge via the Internet at http://pubs.acs.org.

■ AUTHOR INFORMATION

Corresponding Author

dksmith@mail.sdsu.edu

Notes

The authors declare no competing financial interest.

■ ACKNOWLEDGMENTS

This work was supported by the National Science Foundation (CHE-1214151). We thank Joshua Swider (San Diego State University) for help obtaining the mass spectral data.

■ REFERENCES

(1) Huynh, M. H. V.; Meyer, T. J. *Chem. Rev.* **2007**, *107*, 5004−5064.
(2) Weinberg, D. R.; Gagliardi, C. J.; Hull, J. F.; Murphy, C. F.; Kent, C. A.; Westlake, B. C.; Paul, A.; Ess, D. H.; McCafferty, D. G.; Meyer, T. J. *Chem. Rev.* **2012**, *112*, 4016−4093.
(3) Warren, J. J.; Tronic, T. A.; Mayer, J. M. *Chem. Rev.* **2010**, *110*, 6961−7001.
(4) Costentin, C.; Robert, M.; Saveant, J.-M. *Chem. Rev.* **2010**, *110*, PR1−PR40.
(5) Hammes-Schiffer, S.; Stuchebrukhov, A. A. *Chem. Rev.* **2010**, *110*, 6939−6960.
(6) Reece, S. Y.; Nocera, D. G. *Annual Review of Biochemistry*; Annual Reviews: Palo Alto, 2009; Vol. *78*, pp 673−699.
(7) Dempsey, J. L.; Winkler, J. R.; Gray, H. B. *Chem. Rev.* **2010**, *110*, 7024−7039.
(8) Kaila, V. R. I.; Verkhovsky, M. I.; Wikstrom, M. *Chem. Rev.* **2010**, *110*, 7062−7081.
(9) Gust, D.; Moore, T. A.; Moore, A. L. *Acc. Chem. Res.* **2009**, *42*, 1890−1898.
(10) Costentin, C.; Robert, M.; Saveant, J. M. *Acc. Chem. Res.* **2010**, *43*, 1019−1029.
(11) Breinlinger, E.; Niemz, A.; Rotello, V. M. *J. Am. Chem. Soc.* **1995**, *117*, 5379−80.
(12) Gray, M.; Cuello, A. O.; Cooke, G.; Rotello, V. M. *J. Am. Chem. Soc.* **2003**, *125*, 7882−7888.
(13) Gupta, N.; Linschitz, H. *J. Am. Chem. Soc.* **1997**, *119*, 6384−6391.
(14) Gomez, M.; Gonzalez, F. J.; Gonzalez, I. *J. Electrochem. Soc.* **2003**, *150*, E527−E534.
(15) Gomez, M.; Gomez-Castro, C. Z.; Padilla-Martinez, I. I.; Martinez-Martinez, F. J.; Gonzalez, F. J. *J. Electroanal. Chem.* **2004**, *567*, 269−276.
(16) Macias-Ruvalcaba, N. A.; Gonzalez, I.; Aguilar-Martinez, M. *J. Electrochem. Soc.* **2004**, *151*, E110−E118.
(17) Gomez, M.; Gonzalez, F. J.; Gonzalez, I. *J. Electroanal. Chem.* **2005**, *578*, 193−202.
(18) Galano, A.; Gomez, M.; Gonzalez, F. J.; Gonzalez, I. *J. Phys. Chem. A* **2012**, *116*, 10638−10645.
(19) Hui, Y.; Chng, E. L. K.; Chng, C. Y. L.; Poh, H. L.; Webster, R. D. *J. Am. Chem. Soc.* **2009**, *131*, 1523−1534.
(20) Tessensohn, M. E.; Hirao, H.; Webster, R. D. *J. Phys. Chem. C* **2013**, *117*, 1081−1090.
(21) Astudillo, P. D.; Tiburcio, J.; Gonzalez, F. J. *J. Electroanal. Chem.* **2007**, *604*, 57−64.
(22) Alligrant, T. M.; Alvarez, J. C. *J. Phys. Chem. C* **2011**, *115*, 10797−10805.
(23) Medina-Ramos, J.; Alligrant, T. M.; Clingenpeel, A.; Alvarez, J. C. *J. Phys. Chem. C* **2012**, *116*, 20447−20457.
(24) Nijhuis, C. A.; Ravoo, B. J.; Huskens, J.; Reinhoudt, D. N. *Coord. Chem. Rev.* **2007**, *251*, 1761−1780.
(25) Smith, D. K. In *Electrochemistry of Functional Supramolecular Systems*; Ceroni, P., Credi, A., Venturi, M., Eds.; John Wiley: Hoboken, 2010; pp 1−32.
(26) Ge, Y.; Lilienthal, R. R.; Smith, D. K. *J. Am. Chem. Soc.* **1996**, *118*, 3976−7.

(27) Ge, Y.; Miller, L.; Ouimet, T.; Smith, D. K. *J. Org. Chem.* **2000**, *65*, 8831−8838.
(28) Ge, Y.; Smith, D. K. *Anal. Chem.* **2000**, *72*, 1860−1865.
(29) Bu, J.; Lilienthal, N. D.; Woods, J. E.; Nohrden, C. E.; Hoang, K. T.; Truong, D.; Smith, D. K. *J. Am. Chem. Soc.* **2005**, *127*, 6423−6429.
(30) Woods, J. E.; Ge, Y.; Smith, D. K. *J. Am. Chem. Soc.* **2008**, *130*, 10070−10071.
(31) Clare, J. P.; Statnikov, A.; Lynch, V.; Sargent, A. L.; Sibert, J. W. *J. Org. Chem.* **2009**, *74*, 6637−6646.
(32) Clare, L. A.; Rojas-Sligh, L. E.; Maciejewski, S. M.; Kangas, K.; Woods, J. E.; Deiner, L. J.; Cooksy, A.; Smith, D. K. *J. Phys. Chem. C* **2010**, *114*, 8938−8949.
(33) Solis, V.; Iwasita, T.; Giordano, M. C. *J. Electroanal. Chem.* **1976**, *73*, 91−104.
(34) Klymenko, O. V.; Giovanelli, D.; Lawrence, N. S.; Rees, N. V.; Jiang, L.; Jones, T. G. J.; Compton, R. G. *Electroanalysis* **2003**, *15*, 949−960.
(35) "Reversible/irreversible" can be ambiguous in voltammetry, since the terms can be used to refer both to the stability of the product(s) and to the kinetics of the electron transfer. It is clearer to use "chemically" reversible to refer to the stability and "electrochemically" reversible to refer to the kinetics. The former is commonly evaluated by the ratio of peak currents, with a ratio of $i_{p,rev}/i_{p,for} = 1$ for a chemically reversible process, and the latter by the difference in peak potentials, ΔE_p. For CV with freely diffusing species in the absence of IR_u drop this means $\Delta E_p = 60/n$ mV (at 25 °C). However, in this paper, because of significant IR^u drop, we use less rigorous definitions: "electrochemically reversible" is used to describe CV waves in which the oxidation and reduction components occur in the same potential range but may have a $>60/n$ mV ΔE_p due to IR_u drop. "Electrochemically irreversible" indicates CV waves where the oxidation and reduction components are well separated in potential. CV waves which are both chemically and electrochemically reversible by the above definition are simply termed "reversible".
(36) One particularly relevant example is the reduction of flavins in aprotic solvents which are believed to undergo a similar overall reaction as we have proposed for the ureas. In this case, reduction produces a radical anion which can be protonated by an oxidized flavin, resulting in further reduction of the radical and electroinactivation of the deprotonated flavin. The result is a voltammetric peak of $1e^-$ height, but clearly chemically irreversible behavior. See refs 37 and 38.
(37) Tan, S. L. J.; Webster, R. D. *J. Am. Chem. Soc.* **2012**, *134*, 5954−5964.
(38) Niemz, A.; Imbriglio, J.; Rotello, V. M. *J. Am. Chem. Soc.* **1997**, *119*, 887−892.
(39) Anslyn, E. V.; Dougherty, D. A. *Modern Physical Organic Chemistry*; University Science Books: Sausalito, 2006; pp 528−529.
(40) Staib, A.; Borgis, D.; Hynes, J. T. *J. Chem. Phys.* **1995**, *102*, 2487−2505.
(41) Mader, E. A.; Mayer, J. M. *Inorg. Chem.* **2010**, *49*, 3685−3687.
(42) Laviron, E. *J. Electroanal. Chem.* **1981**, *124*, 1−7.
(43) Newman, J. *J. Electrochem. Soc.* **1966**, *113*, 501−2.
(44) LeSuer, R. J.; Buttolph, C.; Geiger, W. E. *Anal. Chem.* **2004**, *76*, 6395−6401.
(45) Dvorak, V.; Nemec, I.; Zyka, J. *Microchem. J.* **1967**, *12*, 324−349.
(46) Quinn, J. R.; Foss, F. W.; Venkataraman, L.; Breslow, R. *J. Am. Chem. Soc.* **2007**, *129*, 12376−12377. The supporting information in this work shows the CVs of a number of phenylenediamine derivatives in acetonitrile, most of which show two reversible waves.
(47) The aqueous pK_a's of the +1 protonated forms of pyridine (5.17) and *N*,*N*′-dimethylaniline (5.15) are nearly identical. See: *Lange's Handbook of Chemistry*, 16th ed.; Speight, J. G., Ed.; McGraw-Hill: New York, 2005. In acetonitrile, pyridine is more basic but the two are within an order of magnitude: pyridine (5.77) and *N*,*N*′-dimethylaniline (4.91). Izutsu, K. *Acid-Base Dissociation Constants in Dipolar Aprotic Solvents*; Blackwell Scientific Publications: Boston, 1990.
(48) Michaelis, L.; Schubert, M. P.; Granick, S. *J. Am. Chem. Soc.* **1939**, *61*, 1981−1992.
(49) Iida, Y.; Matsunaga, Y. *Bull. Chem. Soc. Jpn.* **1968**, *41*, 2535−6.
(50) Nakayama, S.; Suzuki, K. *Bull. Chem. Soc. Jpn.* **1973**, *46*, 3694−8.
(51) Yamaguchi, K.; Matsumura, G.; Kagechika, H.; Azumaya, I.; Ito, Y.; Itai, A.; Shudo, K. *J. Am. Chem. Soc.* **1991**, *113*, 5474−5475.
(52) Kagechika, H.; Azumaya, I.; Yamaguchi, K.; Shudo, K. *Chem. Pharm. Bull.* **1996**, *44*, 460−462.
(53) Kurth, T. L.; Lewis, F. D. *J. Am. Chem. Soc.* **2003**, *125*, 13760−13767.
(54) For more detailed discussion of this, see: Costentin, C.; Hajj, V.; Robert, M.; Saveant, J. M.; Tard, C. *J. Am. Chem. Soc.* **2010**, *132*, 10142−10147.